First results with THGEM followed by submillimetric multiplying gap

PUBLISHED BY IOP PUBLISHING FOR SISSA MEDIALAB

RECEIVED: *March 1, 2013*
ACCEPTED: *May 5, 2013*
PUBLISHED: *June 10, 2013*

First results with THGEM followed by submillimetric multiplying gap

A.E.C. Coimbra,[a,1] **A.S. Conceição,**[a] **J.A. Mir,**[b] **A. Rubin,**[c] **M. Pitt,**[c] **A. Breskin,**[c] **C.A.O. Henriques**[a] **and J.M.F. dos Santos**[a]

[a] *GIAN, Departamento de Física, Faculdade de Ciências e Tecnologia, Universidade de Coimbra, Rua Larga, 3004-516, Portugal*

[b] *Science and Technology Facilities Council, Rutherford Appleton Laboratory, Chilton, Didcot, Oxon, OX11 0QX, U.K.*

[c] *Department of Particle Physics and Astrophysics, Weizmann Institute of Science, 76100, Rehovot, Israel*

E-mail: Aeccoimbra@gian.fis.uc.pt

ABSTRACT: This work presents the first results dealing with THGEMs coupled to submillimetric multiplication gaps, operated in an atmospheric pressure of Ne/CF_4. The experimental studies done so far with a THGEM coupled to submillimetric multiplication gaps achieved charge-gains of 4×10^4 and 1×10^5 in Ne/CF_4 (95:5), for 0.4 mm and 0.8 mm gaps, respectively, values that are one order of magnitude higher than those obtained in single-THGEM configuration and approximately half from those obtained for a cascaded-THGEM configuration. The present studies evaluate the performance operation in terms of the charge-gain characteristics and X-ray energy resolution.

KEYWORDS: X-ray detectors; Micropattern gaseous detectors (MSGC, GEM, THGEM, RETHGEM, MHSP, MICROPIC, MICROMEGAS, InGrid, etc); Electron multipliers (gas); Charge transport and multiplication in gas

[1] Corresponding author.

doi:10.1088/1748-0221/8/06/P06004

2013 JINST 8 P06004

Contents

1 Introduction **1**

2 Electric field simulations **2**

3 Experimental setup and methodology **5**

4 Results in Ne/CF_4 (95:5) **6**
4.1 Charge gain 6
4.2 Energy resolution 8

5 Discussion **9**

2013 JINST 8 P06004

1 Introduction

An electron multiplier design consisting in a GEM [1] coupled to a Micromegas [2], GEM-MIGAS, namely a second multiplying gap of some tens of microns thick, was recently proposed [3, 4]. Charges emerging from the avalanche in the GEM holes are immediately multiplied in this parallel gap. Compared to a cascade of multipliers separated by a transfer region of a few millimetres [5, 6], this design allows a much more efficient extraction of the charge from the GEM into a high-field region, minimizing the loss of electrons to the GEM bottom electrode as well as to the top electrode of the second element in the cascade. This direct coupling resulted in ten-fold higher gains compared to that obtained in a standard single-GEM [7]. In addition, the intense electric field across the parallel gap allows defocusing of the drift lines in this region [8], reducing the avalanche-ion backflow to values similar to that in triple GEM [9] and Single MHSP [10].

In this work, we extend the concept of GEM-MIGAS to the Thick Gas Electron Multiplier, THGEM [11], coupling it to a thin induction gap, of typically a few hundred microns. The THGEM is a ten-fold larger scaled version of the GEM, manufactured typically from PCB-like materials (FR-4 or G-10) copper clad on both sides, with mechanically-drilled holes; a chemical etching results in small rims around the holes (typically 0.02–0.1 mm), to reduce the discharge probability improving the maximal achievable gain by as much as one order of magnitude [12]. The THGEM is robust, simple to manufacture over large areas, and providing gains that are typically an order of magnitude higher when compared to GEMs [13]. Replacing the usual charge-induction gap following the THGEM electrode with a thin multiplication gap, would result in higher charge-gains, reduced ion backflow and faster pulse rise-times — compared to a Single-THGEM. Unlike the GEM-MIGAS, the kapton pillar spacers used to define the induction gap are not required, since the rigid THGEM provides a constant distance from its bottom electrode to the induction anode readout.

The combination of a THGEM and a Micromegas has already been used in a cryogenic gaseous photomultiplier [14] as an alternative to Double-THGEM, for reducing the ion backflow in

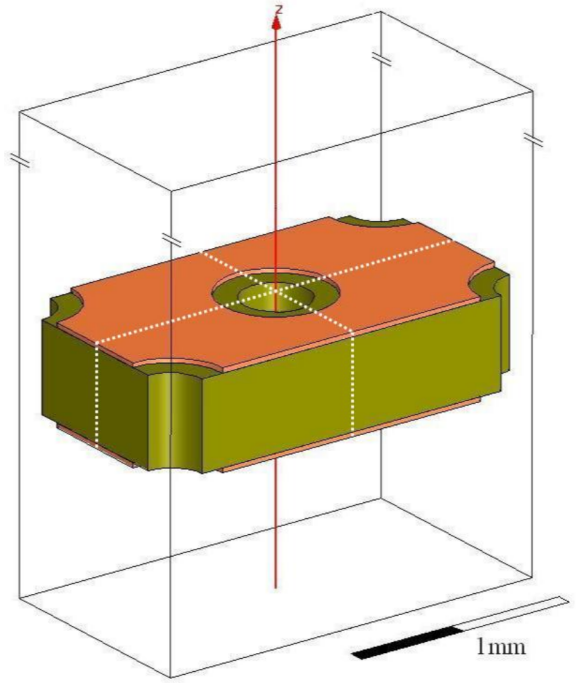

Figure 1. Representation of the three dimensional THGEM cell, highlighting the boundaries (white dotted lines) of the repeated unit cell used in the simulations.

the multiplier cascade. The present configuration provides a similar approach, with the advantage of a more efficient charge transfer between the multiplication stages. In particular, this concept permits to reduce the thickness of the electron multiplier, e.g. a requirement imposed by some experimental constraints. An example is the digital hadron calorimeter (DHCAL) under development for the future ILC-SiD detector [15], requiring a cascade of thinnest-possible sampling elements interlaced with conversion elements. The potential success of the current approach could have some advantage compared to other concepts, including single- and double-THGEM [16].

The results of the present study with soft X-rays provide a preliminary evaluation of the detector's performance, in terms of the charge-gain, energy resolution and stability and in Ne-5% CF_4.

2 Electric field simulations

Electric-field simulations with Ansys release 12 package [17] were carried out to assess and optimize the field strength and distribution in the THGEM/parallel-gap configuration, under various geometrical and bias conditions. They permitted to define the conditions and the region of electron multiplication.

The unit cell shown in figure 1 corresponds to a 4-fold rotation of the basic 1/4 cell along the Z-axis used in the simulations and consisted of a THGEM with the following parameters: 0.4 mm thick G-10 with 0.02 mm thick copper clad on both sides, cylindrical holes of 0.3 mm diameter arranged in a hexagonal pattern with 1 mm pitch and an etched rim around holes of 0.1 mm; the multiplication parallel gap was of either 400 μm or 800 μm deep. The drift/conversion region was set at 11.5 mm.

2013 JINST 8 P06004

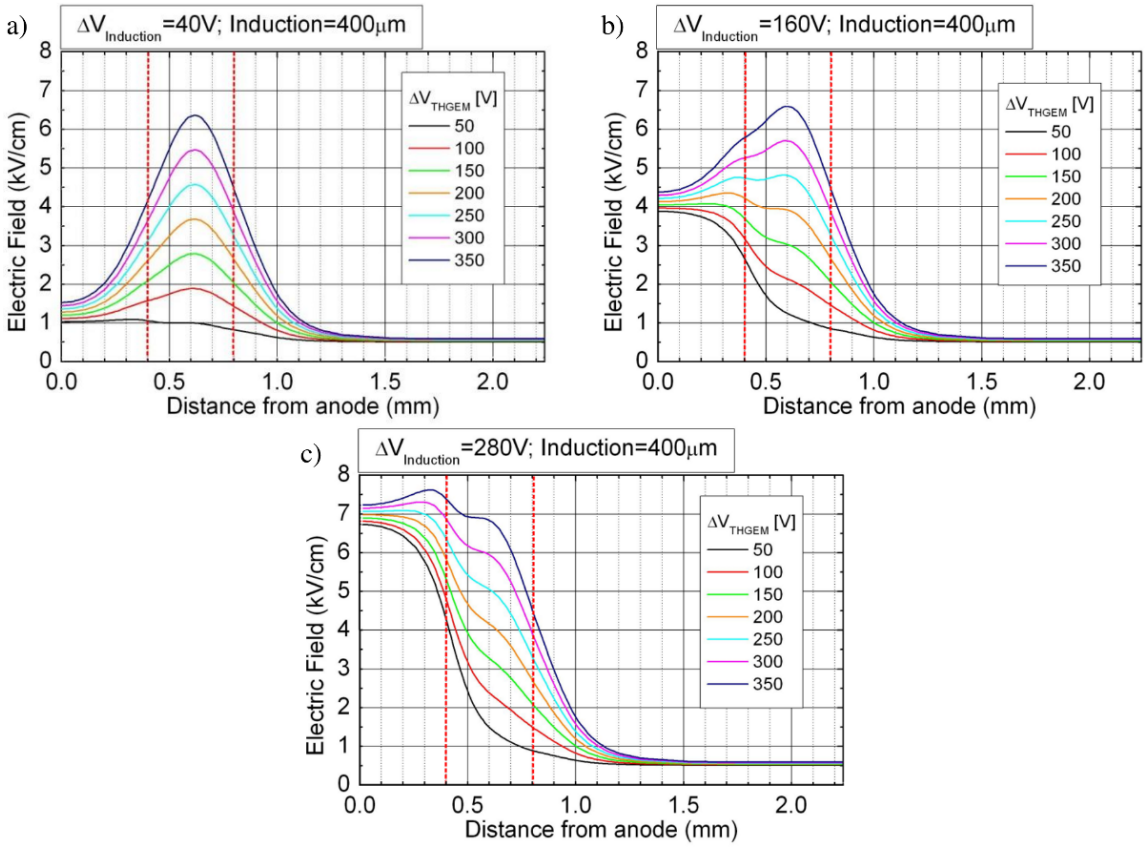

Figure 2. Electric field profile along the axis of a THGEM hole coupled to a multiplication gap of 400 μm, for THGEM voltages in the range of 50 to 350 V; gap voltages: 40 V (a), 160 V (b) and 280 V (c).

The electric-field strength was calculated along the axis of one of the THGEMs holes, i.e. along the Z-axis in figure 1, at different bias settings on the THGEM and for different parallel-gap depths. In all of the following representations the abscissa corresponds to the distance (in mm) from the anode in the multiplication gap, with the origin corresponding to the anode. The drift field was set at constant value of 0.5 kV/cm.

Figure 2 provides the simulation results for a 400 μm gap. In these simulations and for each case the bias voltage on the THGEM was varied in the range 50–350 V,while across the gap the induction voltage was set at 40, 160 and 280 V, corresponding roughly to parallel-gap fields, E_{Gap}, of 1, 4 and 7 kV/cm, respectively. Figure 3 depicts simulation results for an 800 μm induction gap, for induction voltages set in the range 0–280 V and THGEM bias values of 150 V, 250 V and 350 V. The gap voltages were selected so as to roughly correspond to E_{Gap} in the range of 0–3.5 kV/cm in 0.5 kV/cm steps.

The simulation results show an evidence of the interdependence of the hole and the induction electric fields in a region between halfway within the THGEM holes and part of the induction region, just outside the holes, which can extend as far as to 300 μm away. Outside this region the influence of the fields on each other becomes negligible.

2013 JINST 8 P06004

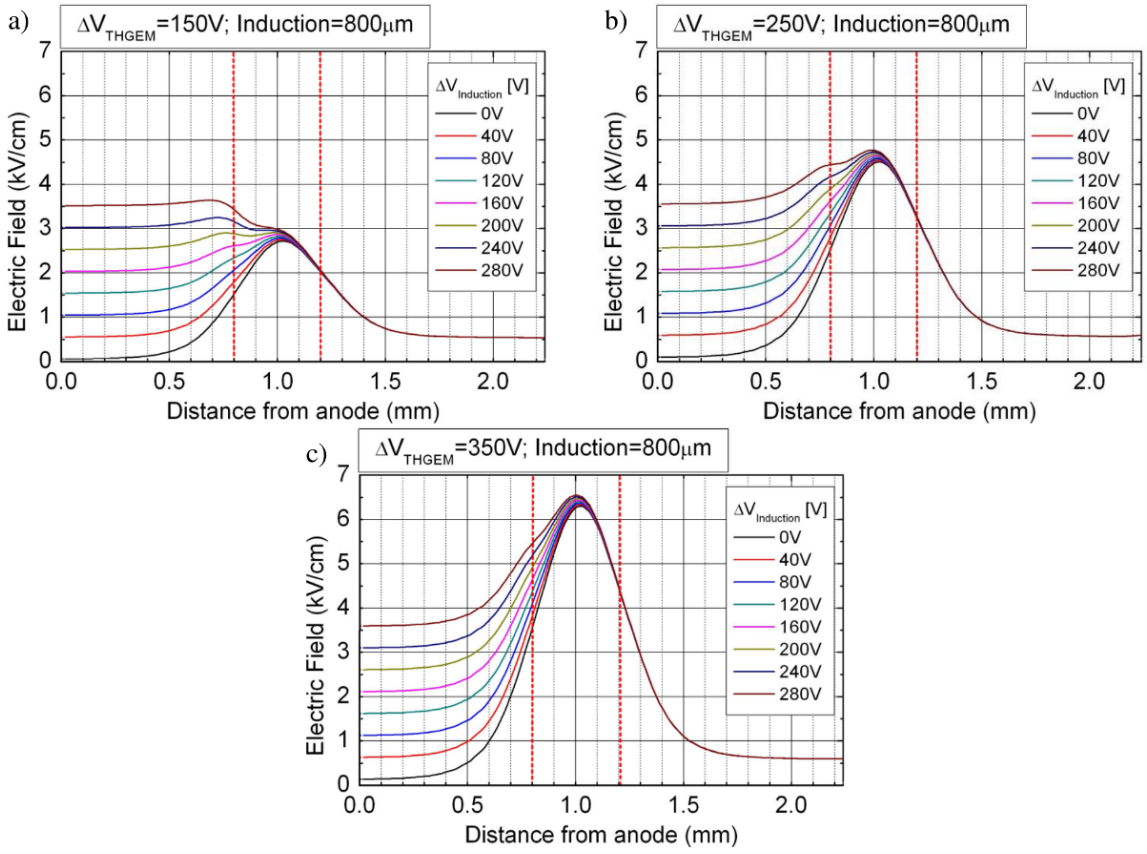

Figure 3. Electric field profile along the axis of a THGEM hole coupled to a multiplication gap of 800 μm, for gap voltages in the range 0 to 320 V and for THGEM voltages of 150 V (a), 250 V (b) and 350 V (c).

For low induction fields, e.g. typical fields of $\sim$ 1 kV/cm, the electric field inside the holes dominates, reaching values of $\sim$ 6.4 kV/cm at the centre of the hole, for typical THGEM voltages of 350 V, presenting a fast decrease when approaching the exit and reducing to values of about 3 and 2 kV/cm at distances of 100 and 200 μm away from the hole exit. We note that in the Ne/5% CF_4 gas mixture used in this work, the onset for gap multiplication was evaluated to be $\sim$ 2 kV/cm [18]. Therefore, if one wants to exploit the full development of the charge avalanche of the THGEM, the induction gap should be thicker than the above values. Nevertheless, even for a distance of 800 μm away from the hole exit there is a slight increase in the induction electric field as the THGEM voltage increases.

As the induction voltage increases, the electric field around the hole exit increases and the charge avalanche extends to outside the holes. Increasing further the voltage in the induction region, the charge avalanche eventually extends to the whole induction region. For high induction voltages, the induction electric field dominates, increasing significantly the field inside the hole, in the region close to the hole exit. Nevertheless, the effect of the induction field becomes smaller towards hole centre, e.g at the hole centre the electric field increases only from 6.4 to 6.8 kV/cm and from 4.5 to 5.0 kV/cm as the induction field near the anode increases from 1 to 7 kV/cm, for a THGEM voltage of 350 V and 250 V, respectively.

2013 JINST 8 P06004

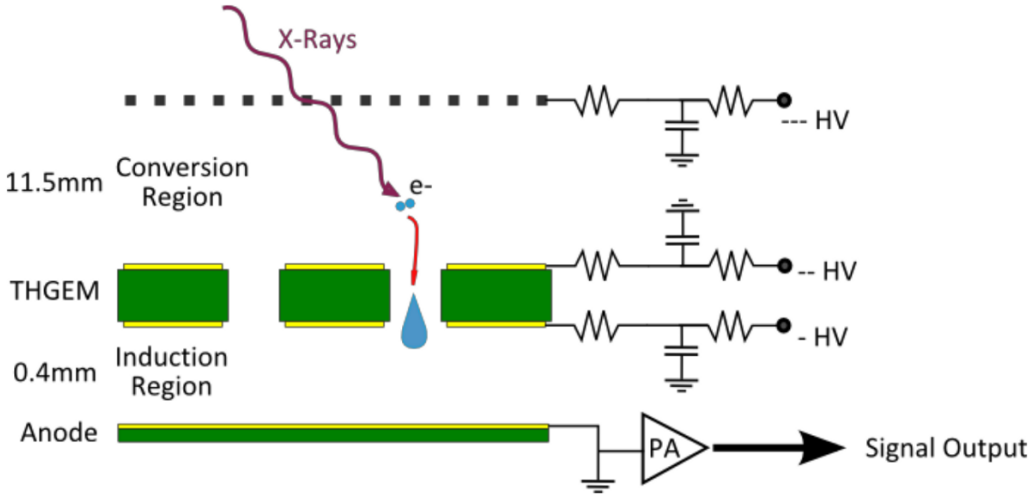

Figure 4. Setup used in pulse-mode measurements. Charges deposited in the drift gap are multiplied in the THGEM; avalanche electrons are further multiplied in the following thin parallel gap.

3 Experimental setup and methodology

For the experimental work, we used a single THGEM produced from G-10 with 0.4 mm thickness and with a 0.02 mm copper clad on both sides. It had a hexagonal pattern of 0.3 mm diameter holes, with a pitch of 1 mm over an active area of 20 mm $\times$ 20 mm; the holes had 0.1 mm wide etched rims.

The THGEM was assembled inside a cylindrical stainless steel vessel ($\sim$ 150 mm in diameter) where in one of the bases a 75 μm thick Kapton window 10 mm in diameter was installed. The Kapton was glued to the chamber with TRA-BOND 2116 low vapour-pressure epoxy. The detector, depicted in figure 4, had a stainless-steel drift mesh, of 50 μm thick wires and with 500 μm pitch, the THGEM and a copper anode plane; it was assembled on Teflon mountings within the stainless steel chamber.

The drift/conversion region was 11.5 mm wide, set by Macor spacers; the induction (multiplication) gap was varied from 400 μm up to 800 μm, using spacers of adequate thickness.

The chamber was vacuum pumped down to 10^{-5} mbar by a turbo-molecular pump and then filled with 1 bar Ne/5% CF_4 mixture. The gases used were research grade Ne 40 (Ne 99.99%) and CF_4 R14 (purity of 99.8%); Ne was filled through a cold finger immersed in liquid nitrogen. After filling, the chamber was decoupled from the gas-filling system and gas purity was maintained by circulating it, by convection, through SAES St707 non-evaporable getters, heated to $\sim$ 150°C.

The detector was irradiated through the Kapton window with 5.9 keV X-rays from a ^{55}Fe source, collimated to 1.5 mm diameter. The resulting primary electron cloud deposited in the 11.5 mm drift region was focused into the THGEM holes where the electrons were multiplied. The avalanche electron cloud was extracted into the following gap where further multiplication occurred under sufficiently high electric field. The resulting electron charge signal was read-out on a copper anode, with a Canberra 2004 charge pre-amplifier with a sensitivity of 0.2 V/pC. The charge signals were also visualized on a digital oscilloscope Tektronix TDS 2022B (200 MHz, 2 GS/s).

2013 JINST 8 P06004

The charge signals were further processed by a Canberra 2025 shaper; pulse-height spectra were recorded with a Maestro Multi-Channel Analyzer. The electronic chain was calibrated for charge gain determination using the 2.2 pC/V test input of the preamplifier and a BNC model PB-3 precision pulse generator.

The drift mesh was biased using an Ortec 659 high-voltage power supply; the THGEM electrodes were biased with a CAEN N471A high-voltage power supply. Voltages were supplied to the respective electrodes through low-pass RC filters with a cutoff frequency of ~ 16 Hz.

4 Results in Ne/CF_4 (95:5)

The pulse-height distributions obtained for the 5.9 keV X-rays were fitted to a Gaussian superimposed on a linear background; the peak centroids and the respective FWHM values were registered for each experimental condition. The detector gain was derived from the centroids, using the electronics calibration.

The chamber was filled with a Ne/CF_4 (95:5) mixture at 1 bar, circulating in the chamber by convection through the getter; measurements were made after at least 24 h of gas purification. The applied drift field was of 0.2 kV/cm. The average counting rate with the X-ray source was of ~ 450 Hz.

4.1 Charge gain

Figure 5a depicts the charge gain measured on the anode as a function of the voltage applied to the THGEM ($\Delta V_{\mathrm{THGEM}}$), for different values of electric field in the multiplication gap (E_{Gap}) (between 1 and 5.7 kV/cm), of 400 μm depth following the THGEM. The limitation on the applied induction field and $\Delta V_{\mathrm{THGEM}}$ was determined by the onset of discharges at a rate of about 0.5 discharges per minute. A gain increase from 7.8×10^3 to 2.2×10^4 was observed for E_{Gap} increase in the multiplying gap from 1 to 5.7 kV/cm. The gain curves show a typical exponential rise; the increase in E_{Gap} showed a shift of the gain-curves to lower THGEM bias values, as previously observed in GEM-MIGAS [7].

Figure 5b presents the gain curves for a multiplication gap of 500 μm. A somewhat larger gain increase with increase of E_{Gap} is observed, compared to the smaller gap: from $\sim 2 \times 10^4$ at 1 kV/cm to 10^5 at 5.6 kV/cm. A thicker induction region allows further development of the electron avalanche. Figure 5c depicts the gain with an 800 μm thick multiplication gap. A maximum gain of $\sim 10^5$ before the onset of microdischarges was obtained with an E_{Gap} of 3.8 kV/cm.

Previous works [13] provided maximum gains in Single-THGEM of $\sim 5 \times 10^3$ and in a Double-THGEM of $\sim 7 \times 10^4$, in the same gas mixture of Ne/CF_4 (95:5). Thus the maximum gains reached during the present studies using the THGEM and submillimetric induction gap multiplication proved to reach about 10 fold higher gains than those with the Single-THGEM detector, and similar to that with a double-THGEM.

In figure 6 the charge gain is depicted as a function of the induction field for different values of the THGEM voltage, for a THGEM followed by an 800 μm thick induction gap. An upper induction-field limit around 3.8 kV/cm was reached before the onset of discharges. The same trend was observed for the 400 and 500 μm thick induction gaps, with field limits around 5.5 kV/cm. The limit on the electric field could be due to avalanche-photon feedback within the induction gap.

2013 JINST 8 P06004

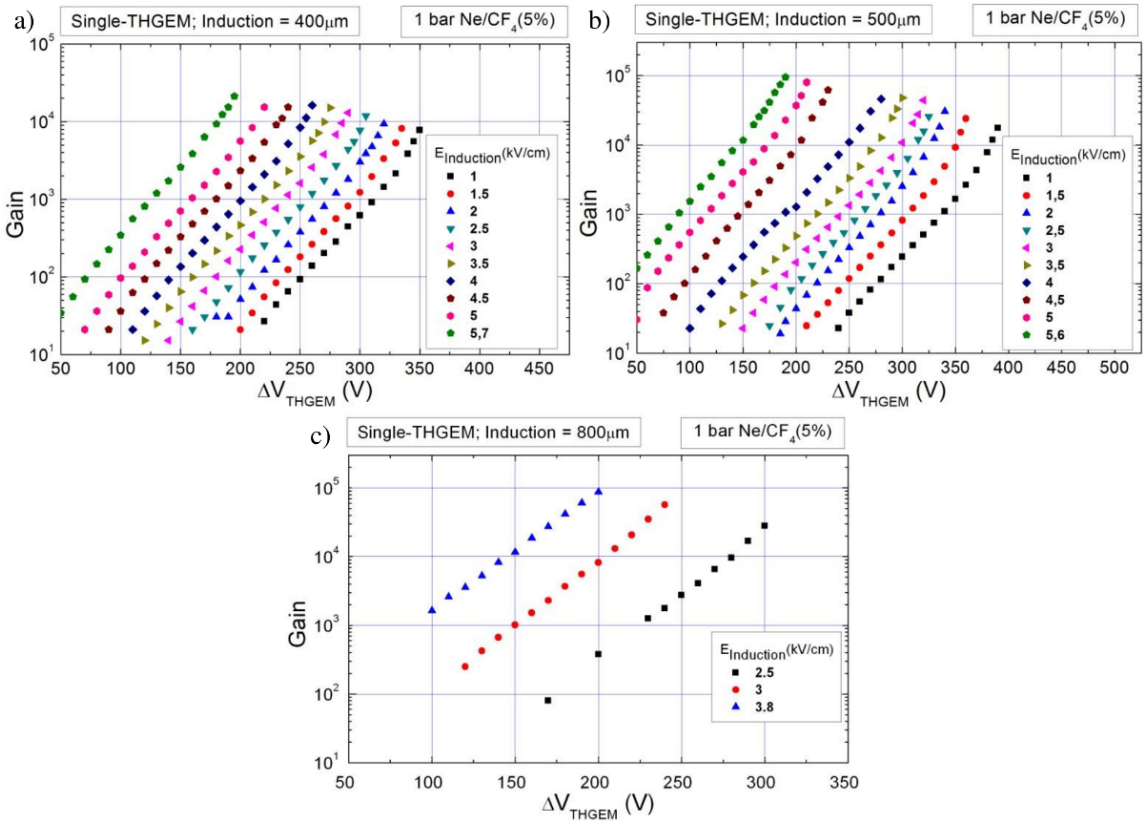

Figure 5. Charge gain as a function of $\Delta V_{\mathrm{THGEM}}$ for different induction fields of the THGEM coupled to induction gaps with thicknesses of: (a) 400 μm, (b) 500 μm and (c) 800 μm.

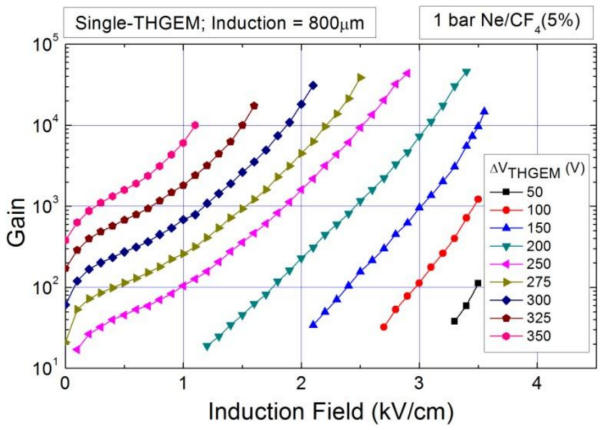

Figure 6. Charge gain as a function of the induction field for different $\Delta V_{\mathrm{THGEM}}$ bias and for 800 μm induction gap.

This process involves UV photons (emitted, or not quenched by CF4) from the gap-avalanche, impinging on the THGEM bottom electrode and releasing photoelectrons. Thinner induction gaps may sustain higher induction fields, possibly due to smaller avalanche development. Therefore, CH_4 should be a more adequate quencher in this detector configuration.

2013 JINST 8 P06004

It can be seen from figure 6 that for low induction fields (lower than ~ 1 kV/cm) there is a gradual increase of charge gain followed by a much steeper increase. This behavior is due, both, to an improved charge collection by the anode (higher electron extraction) and by the onset of gap multiplication. To reach the same gain value for increasing E_{Gap}, the required $\Delta V_{\mathrm{THGEM}}$ was decreased. For example, for the E_{Gap} of ~ 1 kV/cm, the required $\Delta V_{\mathrm{THGEM}}$ to reach gains of 10^4 was on the order of 350 V while for the E_{Gap} of 3.5 kV/cm it was only necessary to apply $\Delta V_{\mathrm{THGEM}}$ of 150 V to reach the same gain values.

The transition from multiplication only inside the hole to multiplication also in the induction region is gradual which indicates that the avalanche region extends to outside of the hole into the induction region.

Figure 6 indicates a ~ 4 fold decrease in maximum gain for $\Delta V_{\mathrm{THGEM}}$ increase from 200 V to 350 V. The maximum applied induction field was simultaneously reduced from ~ 3.5 kV to ~ 1.2 kV/cm, before the onset of occasional sparks. A fairly constant maximum gain could be achieved for a wide range of $\Delta V_{\mathrm{THGEM}}$, between 200 and 300 V and corresponding induction fields between 3.5 and 2.1 kV/cm, respectively.

4.2 Energy resolution

Figure 7 depicts the energy resolution (% FWHM) for 5.9 keV X-rays as a function of the gain, for some values of the induction field, of a THGEM followed by an induction gap of 400 μm (4a), 500 μm (4b) and 800 μm (4c). After an initial fast decrease of the peak width with increasing gain, the energy resolution stabilized between $\sim 25\%$ and $\sim 35\%$ FWHM, degrading at higher gains, due to the onset of photon feedback. A trend observed is that low induction fields resulted in somewhat better energy resolution values, with a broader resolution plateau. The induction-field increase degraded the energy resolution, due to additional statistical fluctuations introduced by the gap multiplication process. In addition, the energy-resolution plateau is shortened and shifted towards higher gains. For the highest induction fields, the best energy resolutions $\sim 30\%$ FWHM were achieved for the 400 μm thick induction gap and $\sim 35\%$ FWHM for the larger gaps. The degradation of these energy resolutions occurred at gains above 1×10^4 with the 400 μm gap and above 6×10^4 for the larger ones, reaching at maximum gains values of 40–45% FWHM.

For comparison, the energy resolution obtained in a Single-THGEM [16] was $\sim 25\%$ FWHM for gains above 10^2, degrading to $\sim 30\%$ FWHM for gains above 2×10^3 and reaching roughly 40% FWHM close to a gain of 5×10^3. In the present configuration, a gain of 2×10^3 yielded energy resolutions of $\sim 27\%$, 25% and 27% FWHM for multiplication gaps of 400, 500 and 800 μm, respectively.

The Double-THGEM setup in [16] yielded the best energy resolution of 25% FWHM at a gain of a few times 10^4. With the 400 μm induction gap this charge gain value was only reached for relatively high induction fields (5.7 kV/cm) with degraded energy resolution ($\sim 45\%$ FWHM) — due to the high amplification in the induction region — while for the other investigated induction gaps lower induction field was required to reach the same gain but with some noticeable energy resolution degradation.

2013 JINST 8 P06004

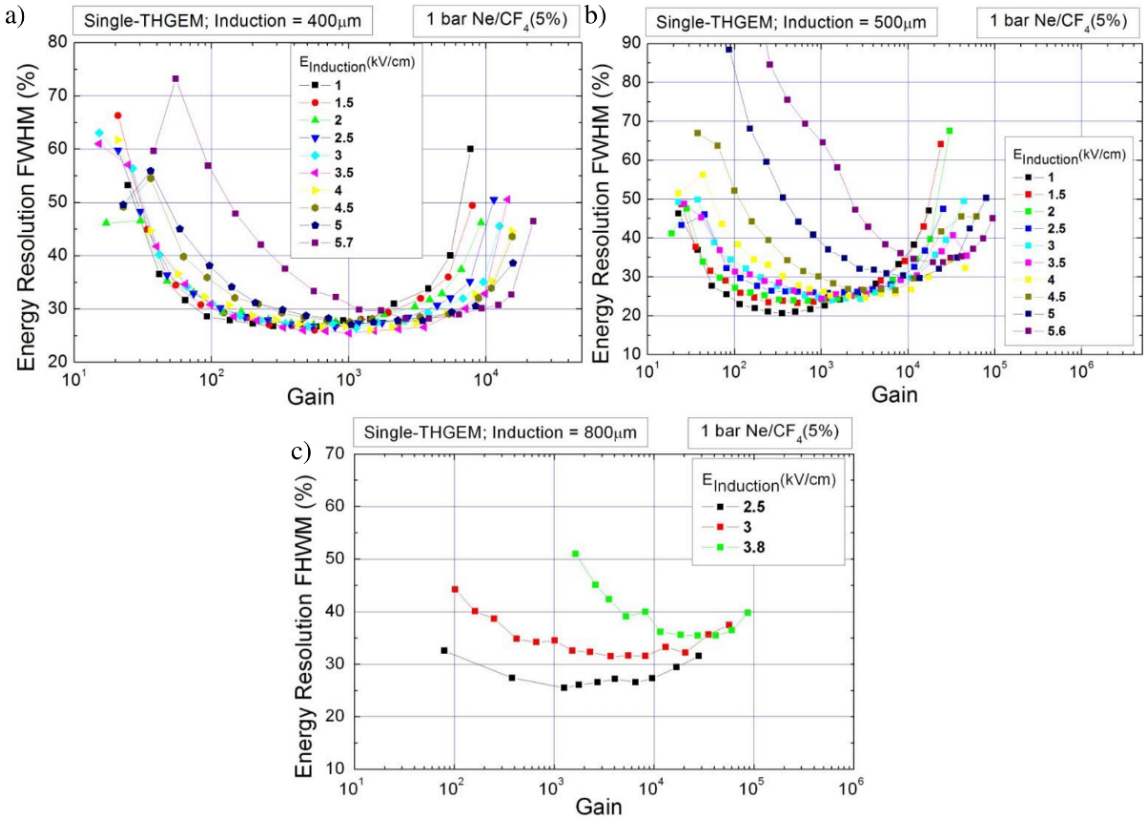

Figure 7. Energy resolution of 5,9 keV X-rays as a function of charge gain for different values of induction fields applied across gaps of 400 μm (a), 500 μm (b) and 800 μm (c).

5 Discussion

The characteristics of THGEM based detectors operated with additional multiplication in a sub-millimeter (400, 500 and 800 μm) induction gap were investigated in Ne/CF_4 (95:5). The charge gain and energy resolution were determined with 5.9 keV X-rays, as function of the applied bias to the THGEM and the induction gap.

Maximum gains of 10^5, similar to those obtained with a standard double-THGEM configuration operated in the same gas mixture, can be reached for induction gaps between 500 and 800 μm. The maximum respective applied gap-fields decreased from $\sim$ 5.5 to $\sim$ 3.8 kV/cm. The maximum gain limitation is due to poor VUV avalanche-photon quenching by CF_4, which also scintillates in the VUV. At higher inductions fields, gain-limiting photon-feedback effects occurs as the electron avalanche extends into the induction gap. Replacing CF_4 by a CH_4 quencher should enable higher gains.

Nevertheless, we have shown that it is possible to conceive a relatively thin electron multiplier capable of reaching high gains. Further investigations are required to evaluate the performance of such thin detector elements with different gases and over larger areas. Compared to a regular THGEM followed with an induction-collection gap yielding fast electron signals, one has to investigate effects due to slower avalanche-ion components on the signals due to the transit of the

2013 JINST 8 P06004

positive ions across the gap. The latter may affect high-rate applications. The present concept may be evaluated as an alternative sampling element for Digital Hadron Calorimeter under development for ILC [15], where the detector thickness plays an important role. The possibility to reach high gains in this detector concept, with relatively lower gains on each of the two elements, will allow the use of low biasing voltages, below the respective maximum limits, thus minimizing the discharge probability.

The electric field profile has been computed for several electrostatic conditions in the 400 μm and 800 μm induction regions using Ansys 3D finite element simulation software. The simulations provided a valuable tool to determine the electric field strength on the several regions of the detector. They show that the full development of the charge avalanche of the THGEM extends into the induction gap for more than 200 μm even for induction electric fields well below the charge multiplication threshold, extending deeper inside the gap as the induction electric field increases. In each of the experimental measurements a clear decrease of the THGEM operation voltages was observed for increasing values of applied induction field accompanied by a significant increase of the charge gain — more significant for larger induction gaps.

Acknowledgments

Support is acknowledged to FCT and FEDER, under COMPETE program, through project CERN/FP/123614/2011.

References

[1] F. Sauli, *GEM: a new concept for electron amplification in gas detectors*, *Nucl. Instrum. Meth.* **A 386** (1997) 531.

[2] Y. Giomataris, P. Rebourgeard, J.P. Robert and G. Charpak, *MicrOMEGAs: a high granularity position sensitive gaseous detector for high particle flux environments*, *Nucl. Instrum. Meth.* **A 376** (1996) 29.

[3] J.A. Mir et al., *Short induction gap gas electron multiplier (GEM) for X-ray spectroscopy*, *Nucl. Instrum. Meth.* **A 573** (2007) 179.

[4] J.A. Mir, A.S. Conceição, H.Y. Al-Shejni, J.F.C.A. Veloso and J.M.F. dos Santos, *GEM-MIGAS: charge gain characteristics for the induction gap in the 50–300 μm range*, *Nucl. Instrum. Meth.* **A 621** (2010) 130.

[5] A. Breskin et al., *The multistep avalanche chamber: a new family of fast, high-rate particle detectors*, *Nucl. Instrum. Meth.* **A 161** (1979) 19.

[6] B. Ketzer, Q. Weitzel, S. Paul, F. Sauli and L. Ropelewski, *Performance of triple GEM tracking detectors in the COMPASS experiment*, *Nucl. Instrum. Meth.* **A 535** (2004) 314.

[7] A.S. Conceição, J.M. Maia, J.A. Mir, L.M.P. Fernandes and J.M.F. dos Santos, *GEM-MIGAS electron multiplier operation in argon-methane mixtures*, *IEEE Trans. Nucl. Sci.* **56** (2009) 2874.

[8] A.S. Conceição, J.A. Mir, J.M. Maia and J.M.F. dos Santos, *Ion back-flow suppression in GEM-MIGAS*, *IEEE Trans. Nucl. Sci.* **57** (2010) 3753.

[9] D. Mörmann, A. Breskin, R. Chechik, P. Cwetanski and B.K. Singh, *A gas avalanche photomultiplier with a CsI-coated GEM*, *Nucl. Instrum. Meth.* **A 478** (2002) 230.

2013 JINST 8 P06004

[10] J.M. Maia et al., *Avalanche-ion back-flow reduction in gaseous electron multipliers based on GEM/MHSP*, *Nucl. Instrum. Meth.* **A 523** (2004) 334.

[11] R. Chechik, A. Breskin and C. Shalem, *Thick GEM-like multipliers — a simple solution for large area UV-RICH detectors*, *Nucl. Instrum. Meth.* **A 553** (2005) 35 [physics/0502131].

[12] C.K. Shalem, R. Chechik, A. Breskin, K. Michaeli and N. Ben-Haim, *Advances in thick GEM-like gaseous electron multipliers. Part II: Low-pressure operation*, *Nucl. Instrum. Meth.* **A 558** (2006) 468 [physics/0601119].

[13] A. Breskin et al., *A concise review on THGEM detectors*, *Nucl. Instrum. Meth.* **A 598** (2009) 107 [arXiv:0807.2026].

[14] S. Duval et al., *Hybrid multi micropattern gaseous photomultiplier for detection of liquid-xenon scintillation*, *Nucl. Instrum. Meth.* **A 695** (2012) 163 [arXiv:1110.6053].

[15] L. Arazi et al., *THGEM-based detectors for sampling elements in DHCAL: laboratory and beam evaluation*, 2012 *JINST* **7** C05011 [arXiv:1112.1915].

[16] A.E. C. Coimbra, A. Breskin and J.M.F. dos Santos, *THGEM operation in high pressure Ne/CF_4*, 2012 *JINST* **7** C02062.

[17] www.ansys.com.

[18] M. Pitt, private communication.

2013 JINST 8 P06004